

# Development of a simulation tool for design and off-design performance assessment of offshore combined heat and power cycles

Mohammad A. Motamed<sup>a\*</sup>, Lars O. Nord<sup>a</sup>

<sup>a</sup> NTNU - The Norwegian University of Science and Technology, Department of Energy and Process Engineering, NO-7491, Trondheim, Norway

\*corresponding author: mohammad.a.motamed@ntnu.no

## Abstract

Ambitious targets for reducing carbon dioxide (CO<sub>2</sub>) emissions are set by Norwegian authorities to address the concerns about global warming. Emission reductions in the offshore heat and power sector can play a role in reaching these targets. Parts of the efforts in industry and academia to reduce offshore emissions are concerned with introducing new design configurations or proposing novel operational strategies for the combined heat and power cycles. Therefore, there is a desire to have a fast and reliable design and assessment tool to be used in the early design stage. Here, a generalized design and performance simulation tool is developed presenting a design point and off-design simulation of the offshore heat and power cycles. It helps the designer provide a fast and accurate thermodynamic assessment of proposed design solutions. The tool has a graphical user interface to facilitate working with the tool with a minimum level of effort and background knowledge from the user. Five part-load control strategies are included in the tool. The tool is verified with available data in the open literature and the results are shown to be in good agreement with the reference data. A combined heat and power cycle is designed and simulated at part-loads as a case study. The cycle includes a gas turbine, a process heat extraction unit, and an organic Rankine bottoming cycle. The simulated performance of the design case in various control strategies is compared showing a 2.5% emission reduction relative to the baseline control strategy.

**Keywords:** Process simulation, Variable area nozzle turbine, Sliding pressure, Offshore heat and power, Organic Rankine cycle, Carbon emission

## 1 Introduction

Norway and Iceland have targeted to cut CO<sub>2</sub> emissions by at least 40% relative to the level from 1990 [1]. Norway has pushed the target further up to 55% under the Paris agreement [1]. Oil and gas extraction activities have the highest share of total CO<sub>2</sub> equivalent emissions in Norway. About 27% of total emissions in 2020 originated from oil and gas installations [2]. A potential solution to reduce CO<sub>2</sub> emission in offshore oil and gas installations is producing extra power from the recovered waste heat of gas turbines (GTs). It was shown in [3] that smaller size gas turbines have the opportunity for higher power recovery from the waste heat per unit of the installed gas turbine power size.

Organic Rankine cycles (ORC) have shown competency for low-footprint power production as the bottoming cycle in offshore installations. They are compact and can operate autonomously with lower operating and maintenance costs relative to steam bottoming cycles [4]. Offshore combined heat and power cycles can be accompanied by renewable

energy sources for carbon-reduced power production. Intermittent availability of renewable energies puts gas turbines and the bottoming cycles in part-load operation for most of their lifetime. Therefore, several efforts are seen in the open literature to further optimize ORCs in the off-design part-load operation. The improvements include the development of new operational strategies, component performance upgrades, finding suitable working fluids, and proposing layout design solutions. It was studied in [3] how different ORC configurations with a heat transfer interloop and recuperators can influence the system performance. An optimization on determining the most appropriate organic working fluid among 39 different candidates is carried out in [5]. The study showed that the optimal ratio of fluid critical temperature to the cycle evaporation temperature lies in the range of 0.93 to 1.02. Manente et al., presented an off-design simulation model to optimize the control strategy in an ORC [6]. They showed that ambient temperature has a great

influence on the cycle performance in air-cooled systems. A thorough insight into how ORC components upgrade can influence the cycle performance is presented in [7].

With the ongoing improvements in the industry and academia on ORC performance, it is desired to have a fast and accurate design and simulation tool for performance assessment of the system in the early stages. A knowledge gap is identified in simulation tools covering different part-load control strategies in a gas turbine – ORC combined cycles. A tool that can provide users with the flexibility to select the configuration and operational strategy. Here an in-house tool is developed to design and simulate an ORC cycle with different part-load control strategies. The tool has three main featuring sections. The design section provides a design tool that enables the designer to have a fast assessment of the ORC in the design point. The parametric study section determines the performance behavior of a designed candidate in the design choice range. The simulation section evaluates the key performance indicators under different control strategies at off-design operation. An arbitrary working fluid is allowed in the tool. Therefore, users can choose among about 100 known working fluids in the library. A calculation of the required area and volume of the heat exchangers is provided to help the designer have a good estimation of the design case footprint.

## 2 Method

The design and simulation algorithm, scientific background, and mathematical formulations are presented. The calculations are based on basic thermodynamic and fluid dynamic principles. The open-source CoolProp package is used as the thermodynamic library to determine the thermodynamic properties of the fluids in each thermodynamic state. CoolProp is a comprehensive and free thermodynamic database that provides a fast and accurate estimation of thermodynamic properties for a wide range of organic fluids [8]. A list of available substances as the working fluid is available on the CoolProp reference list.

The cycle performance is estimated by identifying the thermodynamic states in the intercomponent stations in the cycle. It is known that two independent thermodynamic properties are sufficient to determine the thermodynamic state of a single-phase substance uniquely [9]. Mass flow rate is the third parameter to determine component performance. Therefore, three parameters at each station are necessary and enough to determine a component's performance. Each station is then identified by setting two thermodynamic properties and the mass flow rate passing through that intercomponent point. A pinch point temperature difference (PPTD) approach is taken to design temperatures in the heat exchangers.

### 2.1 System layout configuration

A single spool gas turbine is used as the topping cycle. In a single spool gas turbine, the compressor (COM), the turbine (TUR1), and the electric generator (GEN1) are mounted on the same shaft. Energy is added to the cycle by burning the fuel in the combustion chamber (CC). Process heat is extracted from the gas turbine exhaust at heat exchangers (Hex) before the bottoming cycle waste heat recovery unit. An intermediate heat transfer oil loop is placed between hot gas flow and the ORC to avoid direct contact of oxygen-rich exhaust gas and the organic fluid. A cascade layout is chosen for the combined cycle to avoid power capacity disturbance upon process heat demand change [4]. The exhaust heat then is retracted in a superheater (SUP), an evaporator (EVA), and an economizer (ECO) placed in series to provide heat to the ORC cycle. The ORC cycle is a simple cycle that consists of a variable frequency drive pump, an economizer, an evaporator, a superheater, a throttle valve (in a throttling scenario), and a turbine expander (TUR2), and a condenser (CND). A cooling loop supplied by the sea freshwater is located downstream to absorb the ORC rejected heat. A second electric generator (GEN2) is coupled to the ORC turbine to convert the shaft mechanical power to electric power. Cycle configuration and intercomponent station nomenclatures are illustrated in Fig. 1.

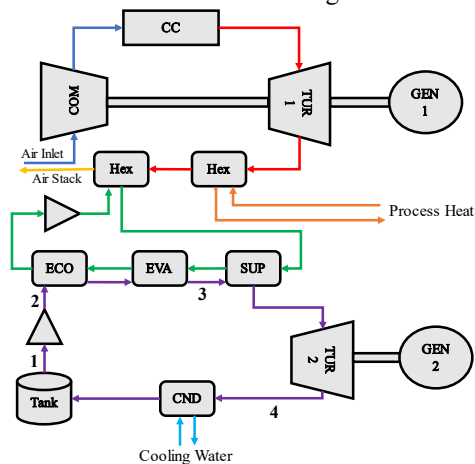


Figure 1: Gas turbine ORC layout configuration. (The abbreviations are explained in the Nomenclature.)

Table 1: Design point input/output list

Input Data	Output Results
Working fluid name	ORC power
Process Heat demand	Working fluid $T_c$
Superheating	ORC pressure ratio
$EGT, \dot{m}_{GT}, \eta_{GT}$	$\eta_{ORC}, \eta_{CC}$
$\eta_{pump}, \eta_{turbine}$	$\dot{m}_{ORC}$
$T_3, T_1, T_{cw}$	$T_{stack}$
$PPTD_{ECO, IOL, CND}$	$\epsilon_{EVA}, \epsilon_{ECO}$
$\Delta P_{ECO, EVA, CND}$	$PPTD_{EVA}$

## 2.2 ORC design tool

The design module in the tool gets the input parameters and provides the user with output results based on the design calculations. Tab. 1 includes the list of required input data and output results. This section includes the sequence of design calculations.

### 2.2.1 Process heat

Hot gas leaving the gas turbine undergoes a constant pressure heat transfer to supply the process heat required by the platform. The amount of needed heat, the exhaust gas mass flow rate, and the exhaust gas temperature are set by the user as inputs. Discharge air properties are calculated based on the conservation of energy law.

### 2.2.2 Intermediate oil heat exchanger

The flue gas then passes through an intermediate oil heat exchanger to transfer the energy from hot air to the ORC working fluid. A temperature drop equal to the allowed PPTD is imposed to determine the oil temperature. Air pressure drops in the heat exchangers are neglected as they do not influence the ORC performance.

### 2.2.3 ORC heat transfer

Heat transfer to the organic fluid is carried out in three main heat exchangers: an economizer, an evaporator, and a superheater (Fig. 1). Evaporation and condensing pressure are determined according to the saturation temperature in the evaporator and condenser.  $P_1, P_2, P_3, P_4$  are then calculated based on the pressure loss values provided by the user as inputs. The thermodynamic cycle is designed to have the working fluid in the liquid saturation phase at the economizer-evaporator interface. Evaporator discharge temperature is elevated by the degree of superheating to set the turbine inlet temperature in the superheated gas region. The cooling water mass flow rate through the condenser is designed for having the allowable PPTD at the condenser's hot side.

### 2.2.4 ORC pump and turbine

Knowing the inlet conditions of the pump and turbine, the discharge thermodynamic properties are calculated based on the isentropic efficiency concept. The pump or turbine discharge enthalpy is determined by knowing the pressure ratio across the component, the isentropic efficiency, and the inlet thermodynamic conditions.

$$h_{out} = h_{in} + (h_{out,s} - h_{in})\eta_s^n \quad (1)$$

Where  $n$  is 1 for a turbine and -1 for a pump.

### 2.2.5 Stack

Flue gas temperature is determined by setting the temperature difference at the economizer cold side to the allowed PPTD value. The organic fluid mass flow rate is adjusted to reach the desired temperature difference at the economizer cold side. Heat transfer effectiveness of the evaporator and the economizer

are calculated by knowing the air temperature on both sides of the heat exchangers.

### 2.2.6 ORC performance

Cycle power output is simply the difference between power generated by the turbine and power consumed by the pump. The turbine/pump power is determined based on energy conservation law and knowing the mass flow rate, inlet, and discharge conditions of the component. Mechanical efficiency and electrical generator efficiency are set to unity in this work but can be adjusted in the code. Cycle thermal efficiency is defined as the ratio of power output to energy input in the cycle. Where delivered energy is calculated from the enthalpy difference between the superheater hot side and the economizer cold side. Finally, the combined cycle efficiency is defined as the ratio of ORC and gas turbine power output divided by the energy input to the system.

$$\eta_{cc} = \eta_{GT} + (1 - \eta_{GT}) \frac{\dot{W}_{ORC}}{\dot{m}_{GT}(h_{EGT} - h_{amb})} \quad (2)$$

### 2.2.7 Heat exchanger size estimation

The heat exchanger's footprint is estimated based on the required effective area for the heat transfer. A generic shell and tube configuration is assumed for the heat exchangers. The generic model proposed in [10], allows for fast design and acceptably accurate performance estimation in the early design stage. The heat exchanger effective area calculation procedure is adapted from [11], [12]. Heat transfer effectiveness is calculated according to the heat exchanger temperatures.

$$\epsilon = \frac{T_{hot,in} - T_{hot,out}}{T_{hot,in} - T_{cold,in}} \quad (3)$$

$$C_{min/max} = \min/\max[C_{cold}, C_{hot}] \quad (4)$$

$$CR = \frac{C_{min}}{C_{max}} \quad (5)$$

$$UA = \frac{C_{min}}{CR - 1} \log\left(\frac{1 - \epsilon}{1 - \epsilon CR}\right) \quad (6)$$

The overall heat transfer coefficient is calculated based on the method suggested in [10], [12] and the Nusselt number, Reynolds number, Prandtl number, and friction factor inside the heat exchanger tubes.

$$Nu = \frac{(Re_D - 10^3)Pr \frac{C_f}{2}}{1.0 + 12.7 \sqrt{\frac{C_f}{2}} (Pr^{2/3} - 1)} \quad (7)$$

$$\alpha = \frac{Nuk}{D} \quad (8)$$

$$U = [\alpha_{hot}^{-1} + \alpha_{cold}^{-1}]^{-1} \quad (9)$$

By knowing the overall heat transfer coefficient, the required effective area is calculated from equations 6 and 9. Afterwards, the width and volume of heat exchangers are estimated according to the effective area needed. It is assumed for the heat exchangers to

have 1000 pipes with 30 mm diameter and 90-micron surface roughness. These assumptions can be changed by the user. The on-design calculation is repeated for various design points upon user request in the parametric study mode. The designed thermodynamic cycle is graphically generated in a temperature-entropy diagram and is shown to the user.

### 2.3 Off-design Simulation

Plant off-design simulation includes performance analysis of the combined cycle in 30%-100% of gas turbine power loads. Gas turbine discharge temperature, mass flow rate, and thermal efficiency are the inputs to the off-design calculations. ORC power output, ORC thermal efficiency, and combined cycle efficiency at the power load range are the output results from the off-design analysis tool. The simulation is carried out for five different ORC control strategies. The simulated control strategies are sliding pressure, throttling valve control, partial admission turbine control, variable area nozzle (VAN) turbine control, and cooling water flow rate control strategies. The five implemented part-load control strategies in the tool are introduced here while a more detailed explanation of their operation principle and background can be reached in [13].

#### 2.3.1 Control strategies

A controller with a sliding pressure strategy uses a variable speed pump that adjusts the cycle flow rate by manipulating the pump's rotational speed. The evaporation pressure slides to match the cycle with reduced heat available to the ORC in part-loads.

A VAN turbine has pivoted vanes as stator blades in the turbine stationary part. In this strategy, the evaporation pressure is kept as high as possible in the part-loads by adjusting the turbine vanes setting angle and modifying the turbine performance without blockage losses [14]. Partial admission turbine control logic has the same strategy as with variable area nozzle except that the mass flow rate admitted to the turbine is regulated by changing the turbine inlet annulus area [15]. The VAN turbine control strategy shows higher part-load cycle efficiency than the partial admission turbine strategy due to less aerodynamic pressure loss in the turbine inlet passage throughflow [16].

The throttling part-load control strategy uses a throttle valve placed at the evaporator discharge to regulate the pressure of the flow entering the turbine. The turbine inlet pressure and mass flow rate are reduced simultaneously in part-load to adjust the ORC power output according to the waste heat available from the gas turbine.

In the cases where a gap exists between the ORC condensing temperature and the supply cooling water temperature in the design point operation, a cooling flow adjustment can be used to allow more efficient power regulation in part-load. Despite the previously mentioned control strategies, the cooling

flow control logic can accompany various control logics to further boost the part-load ORC efficiency. The off-design simulator is an optimizer that finds the optimal thermodynamic cycle in each off-design operational condition. The optimization target is set to be the plant combined-cycle thermal efficiency but can be easily changed to ORC power output, ORC thermal efficiency, or any other desired figure of merits. The optimizer undergoes a simple plane search between all possible manipulating parameters to find the optimal operating point in each off-design condition. In each part-load condition, an ORC cycle is established including the thermodynamic state and the mass flow rate at all intercomponent stations, and the corresponding setting variables in the controller. The number of manipulating parameters is three in the cooling flow control strategy, two in variable area nozzle and partial turbine control strategies, and one in the throttling and sliding pressure control strategy. The cycle mass flow rate is a manipulating parameter in all mentioned control strategies. The cycle pressure ratio is the second setting parameter in the control logic with more than one degree of freedom. Condensing temperature is the third manipulating parameter used in the cooling flow rate control strategy.

#### 2.3.2 Heat exchangers performance

Off-design pressure drop and heat transfer effectiveness in the heat exchangers deviates from the design values in part-load operation and are simulated based on the method presented in [13]. A  $\beta$  parameter is introduced which accounts for the change in the heat transfer coefficient of a heat exchanger [17]. The shift in heat transfer coefficient is calculated according to the change in flow Nusselt number and the fluid conductivity.

$$\beta = \left(\frac{Nu}{Nu_{dp}}\right)\left(\frac{k}{k_{dp}}\right) \quad (10)$$

$$\frac{U}{U_{dp}} = \frac{2\beta_{cold}\beta_{hot}}{\beta_{cold} + \beta_{hot}} \quad (11)$$

#### 2.3.3 Turbine off-design performance

Turbine off-design performance prediction is a calculation of turbine pressure ratio and isentropic efficiency for given mass flow rate, inlet flow conditions, and rotational speed. To accomplish the analysis in given off-design working conditions, a performance map is introduced for each turbine geometry. It is a graphical diagram that illustrates the quantitative relation between four non-dimensional parameters determining the turbine performance [18].

A generalized turbine performance map is used since very little geometrical information is available in the early design stage. The turbine performance map and the pump performance map are adapted from [19] and [20], respectively. The performance maps are normalized and scaled to the design mass flow rate and pressure ratio values. This approach offers flexibility to designers for locating the design

point locating in the performance map. In this work, a choke margin is defined to parametrize the location of the turbine design point in the design speed line of the turbine performance map. Choke margin is defined as the ratio of the mass flow rate difference between the design point and maximum mass flow rate in the design speed line over the difference between maximum and minimum mass flow rates in the design speed line.

A generalized turbine efficiency model is presented in [21] for radial turbines and is used here. Turbine performance change due to adjusting the setting angle in the variable nozzle vanes is modelled in [19] for the range of 20% to 144% of vanes opening angle. The required turbine vane opening angle in each part-load condition is determined based on the desired mass flow rate and pressure ratio through the turbine. Afterwards, the variable area nozzle turbine isentropic efficiency is calculated using the specific speed parameter, the setting value for the vanes opening angle and the model presented in [19]. Specific speed is a well-known indicator for turbomachines which accounts for a combination of mass flow rate and pressure rise.

$$Ns = \frac{NQ^{1/2}}{\Delta h_s^{3/4}} \quad (12)$$

Partial admission turbine efficiency at off-design conditions is simulated based on the method presented in [13]. The throttle valve performance placed before the turbine is predicted according to the method presented in [13] where a constant enthalpy pressure reduction is considered in the valve.

#### 2.3.4 Off-design solver algorithm

The algorithm of the off-design solver is introduced here. A design point calculation is carried out before starting an off-design analysis. Therefore, design data required in the off-design analysis would be available to the solver. The off-design optimization is a plane search over all possible sets of manipulating parameters and then picking up the optimal one by comparing them to all other sets of target outputs. An n-dimensional array of manipulating parameters is set representing the possible options of the controller setting in different control strategies. Where n is the controller degree of freedom in each control strategy. Tab. 2 represents the list of manipulating parameters for the studied control strategies.

Table 2: manipulating variables as the controller setting

Control strategy	Manipulating parameters
Sliding pressure	$\dot{m}_{pump}$
Throttling valve	$\dot{m}_{pump}$
Partial admission turbine	$\dot{m}_{pump}; PR_{turb}$
VAN turbine	$\dot{m}_{pump}; PR_{turb}$
Cooling flow	$\dot{m}_{pump}; PR_{turb}; T_{CND}$

Evaporation and condensing temperature/pressure are determined using the pressure ratio value and assuming no change in the condensing temperature; except for the cooling flow rate control strategy where the condensing temperature is set by the controller. The pump discharge pressure is calculated based on the modified pressure loss in the heat exchangers. The pump outlet temperature is identified using the pump isentropic efficiency resulting from the pump performance map. The economizer hot/cold side temperatures are calculated according to the modified heat transfer coefficient of the heat exchangers. The implicit equations for heat exchanger's inlet/outlet temperatures require an iterative approach to solve. The trial-and-error method is used for this iterative solver. After determining the heat exchanger's temperatures, turbine inlet conditions are calculated accordingly. With all thermodynamic states and mass flow rates known, ORC performance (power output and thermal efficiency) is calculated.

#### 2.4 Software framework

The simulation process is implemented as an in-house code in MATLAB [22]. A user interface is integrated into the code to facilitate using the tool for the users. The inputs can be fed into the tool both through a graphical table interface and through a data file. The user has the option to save and load both input data and results for a more convenient operation with the tool. Gas turbine off-design input data is delivered to the tool in the form of an Excel spreadsheet.

#### 2.5 Tool verification

The validity of the tool is assessed by checking the output results against available data in the open literature. Simulation results are compared with the information presented in [23]. The verification is carried out in the rated power and 50% power load. In the reference work, A Solar Centaur 50 gas turbine is working as the topping cycle and an ORC operates as the bottoming cycle. Two different organic fluids are covered in the verification process to check the dependency of the results on the working fluid. The verification data are tabulated in Tab. 3 showing approximately 1% relative error in the results. Therefore, it could be inferred that the simulation tool results are in good agreement with openly published data in the literature.

#### 2.6 Case study

The developed tool is named ORCSIM and is used to design and simulate a combined cycle. SGT800 gas turbine is considered as the topping cycle on the platform. The gas turbine load is controlled using compressor variable guide vanes to prevent drastic decay of exhaust heat temperature at part-load. 8 MW heat is extracted at the gas turbine discharge to provide the heat demand on the platform. Cyclopentene is the selected working fluid for the ORC since it has suitable pressure values in the range of operating temperatures.

Table 3 Simulation tool verification

Parameters	Verification cases		
	Case 1	Case 2	Case 3
gas turbine load [%]	100	100	50
ORC working fluid	MDM2	Toluene	Toluene
EGT [°C]	520	520	358
$\dot{m}_{GT}$ [kg/s]	19.2	19.2	19.2
$\eta_{GT}$ [% LHV]	28.9	28.9	23.8
$\eta_{ORC}$ , open literature [%]	17.1	27.8	26.7
$\eta_{ORC}$ , current study [%]	17.2	27.9	27.0
relative error [%]	0.5	0.3	1.1

Design assumptions and input data to the design case are adopted from the design case in [13] except for the PPTD in the heat exchangers which is set to 15°C for a lower footprint on the platform. A parametric study is conducted to find the optimal design point based on higher power capacity and lower footprint. Afterwards, an off-design simulation is conducted on the designed combined cycle to assess the cycle performance in part-load with the presented control strategies.

### 3 Results and Discussion

Fig. 2 and Fig. 3 show how the power capacity of the ORC and total heat exchangers volume per MW vary with different design temperatures in the subjected design case, respectively. The design evaporation and condensing temperature are selected from the parametric study to be 200°C and 50°C, respectively. The designed cycle is shown to have the ability to provide 3.4 MW of power with 18.1% thermal efficiency at the design point. The required total volume and total effective heat transfer area of the heat exchangers are estimated to be 1100 m<sup>3</sup> and 4200 m<sup>2</sup> for the design case, respectively.

The simulations showed near-constant thermal efficiency at off-design loads with VAN turbine control logic and cooling flow control logic. However partial admission turbine control strategy, sliding pressure strategy, and throttling control strategy experienced higher efficiency loss relative to the VAN turbine control strategy. The plant with VAN turbine as the ORC expander showed to have a 1.25 percentage point higher combined cycle efficiency at 50% gas turbine load. It will result in 2.5% less CO<sub>2</sub> emission at part-load operation.

### 4 Summary and Conclusions

An in-house design and simulation tool was developed to facilitate the design procedure and an early performance assessment of GT-ORC combined cycles. The tool offers a graphical user interface for a more convenient design experience. Background scientific principles, mathematical formulations, and the coding algorithm were explained. A sample case was designed, and the part-load performance was discussed according to the results from the simulation tool. Five control strategies for off-design power demands were

studied. VAN turbine control strategy showing higher thermal efficiency can be a potential solution for reducing carbon emission on the offshore oil and gas platforms as it reduced the CO<sub>2</sub> emission by 2.5% at part-load operation.

ORC part-load thermal efficiency of the subjected design case is illustrated in Fig. 4. VAN turbine control strategy outperformed other studied control strategies by higher thermal efficiency at part-load.

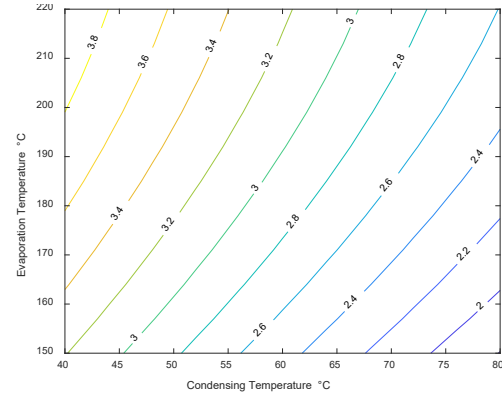


Figure 2: ORC power output design study [MW]

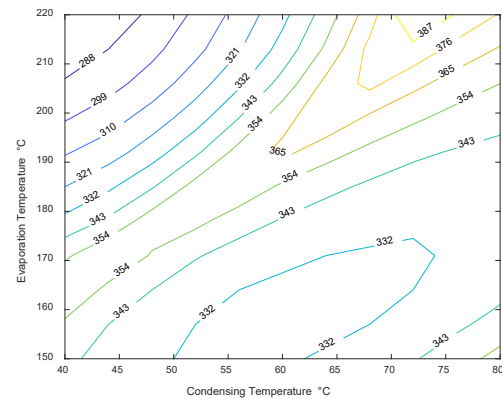


Figure 3 Heat recovery unit specific volume [lit/kW]

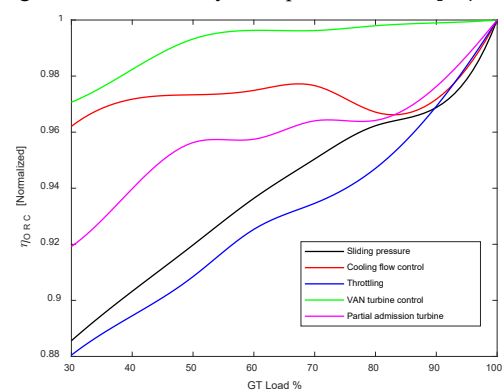


Figure 4: ORC part-load efficiency

### Acknowledgement

This publication has been produced with support from the LowEmission Research Centre (www.lowemission.no), performed under the Norwegian research program PETROSENTER. The authors acknowledge the industry partners in LowEmission for their contributions and the Research Council of Norway (296207).

**Nomenclature**

$A$	heat exchanger effective area ( $m^2$ )
$C$	heat capacity ( $J/K$ )
$CR$	heat exchanger heat capacity ratio
$c_f$	skin friction factor
$D$	diameter (m)
$h$	enthalpy ( $J/kg$ )
$k$	thermal conductivity ( $W/mK$ )
$\dot{m}$	mass flow rate ( $kg/s$ )
$n$	exponent in the efficiency formula
$N$	rotational speed ( $rad/s$ )
$Nu$	Nusselt number
$Ns$	turbine specific speed
$P$	pressure (Pa)
$Pr$	Prandtl number
$Q$	volume flow rate
$Re$	Reynolds number
$T$	temperature (K)
$U$	overall heat transfer coefficient ( $W/m^2K$ )
$\dot{W}$	power (W)

**Greek letters**

$\alpha$	convective heat transfer coefficient
$\beta$	heat transfer ratio coefficient
$\eta$	efficiency
$\epsilon$	heat transfer effectiveness

**Abbreviations**

CC	combustion chamber
CND	condenser
COM	compressor
ECO	economizer
EGT	gas turbine exhaust temperature
EVA	evaporator
GEN	generator
GT	gas turbine
Hex	heat exchanger
ORC	organic Rankine cycle
PPTD	pinch point temperature difference
PR	pressure ratio
SUP	superheater
TUR	turbine

**Subscripts**

$1$	ORC pump inlet
$2$	economizer inlet
$3$	Evaporator outlet
$4$	Turbine outlet
$amb$	ambient
$c$	critical
$cc$	combined cycle
$cold$	heat exchanger cold side
$cw$	cooling water supply
$D$	based on diameter
$dp$	design point

$hot$	heat exchanger hot side
$in$	inlet
$IOL$	intermediate oil loop
$max$	maximum
$min$	minimum
$out$	outlet
$pump$	related to pump
$s$	isentropic
$turbine$	related to turbine

**References**

- [1] NPD, "Exploration Resource report 2020," pp. 1–77, 2020, [Online]. Available: <https://www.npd.no/en/facts/publications/reports2/resource-report/>.
- [2] "Emissions to air," *Statistics Norway*, 2021. <https://www.ssb.no/en/natur-og-miljo/forurensning-og-klima/statistikk/utslipp-til-luft>.
- [3] R. K. Bhargava, M. Bianchi, L. Branchini, A. De Pascale, and V. Orlandini, "Organic rankine cycle system for effective energy recovery in offshore applications: A parametric investigation with different power rating gas turbines," *Proc. ASME Turbo Expo*, vol. 3, 2015, doi: 10.1115/GT2015-42292.
- [4] H. Nami, I. S. Ertesvåg, R. Agromayor, L. Riboldi, and L. O. Nord, "Gas turbine exhaust gas heat recovery by organic Rankine cycles (ORC) for offshore combined heat and power applications - Energy and exergy analysis," *Energy*, vol. 165, pp. 1060–1071, 2018, doi: 10.1016/j.energy.2018.10.034.
- [5] I. Encabo Cáceres, R. Agromayor, and L. O. Nord, "Thermodynamic Optimization Of An Organic Rankine Cycle For Power Generation From A Low Temperature Geothermal Heat Source," *Proc. 58th Conf. Simul. Model. (SIMS 58) Reykjavik, Iceland, Sept. 25th – 27th, 2017*, vol. 138, pp. 251–262, 2017, doi: 10.3384/ecp17138251.
- [6] G. Manente, A. Toffolo, A. Lazzaretto, and M. Paci, "An Organic Rankine Cycle off-design model for the search of the optimal control strategy," *Energy*, vol. 58, pp. 97–106, 2013, doi: 10.1016/j.energy.2012.12.035.
- [7] M. Astolfi, "Technical options for organic rankine cycle systems," in *Organic Rankine Cycle (ORC) Power Systems: Technologies and Applications*, no. 1, 2017, pp. 67–89.
- [8] I. H. Bell, J. Wronski, S. Quoilin, and V. Lemort, "Pure and pseudo-pure fluid thermophysical property evaluation and the open-source thermophysical property library CoolProp," *Ind. Eng. Chem. Res.*, vol. 53, no. 6, pp. 2498–2508, 2014.

- [9] M. J. Moran, H. N. Shapiro, D. D. Boettner, and M. B. Bailey, *Fundamentals of Engineering Thermodynamics, 8th Edition*. Wiley, 2014.
- [10] B. A. L. Hagen, M. Nikolaisen, and T. Andresen, "A novel methodology for Rankine cycle analysis with generic heat exchanger models," *Appl. Therm. Eng.*, vol. 165, no. March 2019, p. 114566, 2020, doi: 10.1016/j.applthermaleng.2019.114566.
- [11] P. L. Dhar, *Thermal System Design and Simulation*. 2016.
- [12] F. Ceglia, E. Marrasso, C. Roselli, and M. Sasso, "Effect of layout and working fluid on heat transfer of polymeric shell and tube heat exchangers for small size geothermal ORC via 1-D numerical analysis," *Geothermics*, vol. 95, no. February, p. 102118, 2021, doi: 10.1016/j.geothermics.2021.102118.
- [13] M. A. Motamed and L. O. Nord, "Assessment of organic rankine cycle part-load performance as gas turbine bottoming cycle with variable area nozzle turbine technology," *Energies*, vol. 14, no. 23, 2021, doi: 10.3390/en14237916.
- [14] C. Liu and T. Gao, "Off-design performance analysis of basic ORC, ORC using zeotropic mixtures and composition-adjustable ORC under optimal control strategy," *Energy*, vol. 171, pp. 95–108, 2019, doi: 10.1016/j.energy.2018.12.195.
- [15] D. Casartelli, M. Binotti, P. Silva, E. Macchi, E. Roccaro, and T. Passera, "Power Block Off-design Control Strategies for Indirect Solar ORC Cycles," *Energy Procedia*, vol. 69, pp. 1220–1230, 2015, doi: 10.1016/j.egypro.2015.03.166.
- [16] M. A. Motamed and L. O. Nord, "IMPROVING THE OFF-DESIGN EFFICIENCY OF ORGANIC RANKINE BOTTOMING CYCLE BY VARIABLE AREA NOZZLE TURBINE TECHNOLOGY," 2021, doi: 10.14459/2021mp1632935.
- [17] N. M. Phu and N. T. M. Trinh, "Modelling and experimental validation for off-design performance of the helical heat exchanger with LMTD correction taken into account," *J. Mech. Sci. Technol.*, vol. 30, no. 7, pp. 3357–3364, 2016, doi: 10.1007/s12206-016-0645-0.
- [18] H. I. H. Saravanamuttoo, G. F. C. Rogers, and H. Cohen, *Gas turbine theory*. Pearson Education, 2001.
- [19] P. L. Meitner and A. J. Glassman, "Off-Design Performance Loss Model for Radial Turbines with Pivoting, Variable-Area Stators.," NATIONAL AERONAUTICS AND SPACE ADMINISTRATION CLEVELAND OH LEWIS RESEARCH CENTER, 1980.
- [20] D. Hu, S. Li, Y. Zheng, J. Wang, and Y. Dai, "Preliminary design and off-design performance analysis of an Organic Rankine Cycle for geothermal sources," *Energy Convers. Manag.*, vol. 96, pp. 175–187, 2015, doi: 10.1016/j.enconman.2015.02.078.
- [21] B. A. L. Hagen, R. Agromayor, and P. Nekså, "Equation-oriented methods for design optimization and performance analysis of radial inflow turbines," *Energy*, vol. 237, p. 121596, 2021, doi: 10.1016/j.energy.2021.121596.
- [22] "MATLAB version R2020b." The MathWorks Inc, 2020.
- [23] J. M. Muñoz De Escalona, D. Sánchez, R. Chacartegui, and T. Sánchez, "Part-load analysis of gas turbine & ORC combined cycles," *Appl. Therm. Eng.*, vol. 36, no. 1, pp. 63–72, 2012, doi: 10.1016/j.applthermaleng.2011.11.068.